

PACS numbers: 79.20.Ds; 79.20.Eb; 42.55.Wd
DOI: 10.1070/QE2014v044n08ABEH015496

Modelling of micromachining of human tooth enamel by erbium laser radiation

A.V. Belikov, A.V. Skrypnik, K.V. Shatilova

Abstract. **We consider a 3D cellular model of human tooth enamel and a photomechanical cellular model of enamel ablation by erbium laser radiation, taking into account the structural peculiarities of enamel, energy distribution in the laser beam cross section and attenuation of laser energy in biological tissue. The surface area of the texture in enamel is calculated after its micromachining by erbium laser radiation. The influence of the surface area on the bond strength of enamel with dental filling materials is discussed. A good correlation between the computer simulation of the total work of adhesion and experimentally measured bond strength between the dental filling material and the tooth enamel after its micromachining by means of YAG:Er laser radiation is attained.**

Keywords: *photomechanical cellular model, ablation, micromachining, erbium laser, human tooth enamel, adhesion.*

1. Introduction

Laser radiation is widely used in modern dentistry [1–3]. Erbium lasers are employed for treatment of hard tissues of the tooth, in particular, for preparation of the tooth surface for sealing the cavities [1–11]. Several studies have reported that the adhesion of the modern filling materials to the surface having been subjected to the laser exposure exceeds the adhesion to the surface formed by conventional tools [4–7]. However, there are reports that suggest the opposite [8–11]. It is obvious that this issue requires further study.

The authors of paper [4] describe the results of experimental study of adhesion of modern filling materials to the enamel surface formed as a result of micromachining by radiation from a YAG:Er-laser. The essence of the micromachining is to create a regular texture of craters on the surface of hard tooth tissue. It is shown that the micromachining significantly increases adhesion, obviously at the expense of increasing the surface area in the texture.

It should be noted that the experimental study of adhesion is extremely laborious. In this connection, the development of a model to describe the behaviour of the enamel's surface area after its laser micromachining is an urgent task.

The authors of papers [12–14] have reported the creation of a photomechanical cellular model of ablation of the human tooth enamel by means of erbium laser radiation. The model proposed takes into account the structural peculiarities of enamel, energy distribution in the laser beam cross section (Gaussian distribution) and attenuation of the laser energy in tissue according to the Bouguer–Lambert–Beer law. The model takes into account the explosive mechanism of laser ablation of hard tooth tissue [15] in case of irradiation by erbium lasers, which is largely absorbed by water (μ_a = 12250 cm^{-1} [16], λ = 2.94 μm) contained in the enamel or dentin of the tooth and to a lesser degree – by hydroxyapatite (μ_a = 300 cm^{-1} [16], λ = 2.94 μm).

This paper represents the results of modelling the texture surface area in the enamel, derived in the framework of a three-dimensional cellular model describing the photomechanical ablation of the human dental enamel by radiation from an erbium laser. We investigate the contribution of microrelief and the distances between the centres of craters into the total surface area of the texture formed as a result of laser irradiation. The interrelation between the texture surface obtained in the calculation and the results of experimental study on the adhesion of the dental filling material Revolution (Kerr, Germany) to the enamel surface treated with YAG:Er-laser radiation is discussed.

2. Cellular model of the human tooth enamel

By volume, the human tooth enamel consists to 87% of minerals (apatite), 11% – of water (free and bound, located inside the pores) and 2% – of an organic matrix [17]. The main structural elements of the tooth enamel are the enamel prisms [18]. Belikov et al. [13] describe the cellular model of the dental enamel, according to which it represents a set of similar elements (cells), evenly distributed in the volume and being in perfect mechanical and optical contact. This model is presented in Fig. 1. Each cell models an enamel prism and consists of two cubes: a cube of hydroxyapatite (HA-cube) and a cube of water (W-cube), the latter symmetrically located within the HA-cube and comprising 11% of the cell volume [17]. The edge length of the HA-cube (L_{HA}) is equal to 5.0 μm (which corresponds to the enamel prism size [18]), the edge length of the W-cube (L_w) is equal to 2.4 μm.

3. Photomechanical cellular model of ablation of the human tooth enamel by erbium laser radiation

This model does not take into account the scattering of light in the enamel and the reflection from its surface, inasmuch as they are insignificant for the lasing wavelengths of erbium

A.V. Belikov, A.V. Skrypnik, K.V. Shatilova St. Petersburg National Research University of Information Technologies, Mechanics and Optics, Kronverkskiy prosp. 49, 197101 St. Petersburg, Russia; e-mail: meddv@grv.ifmo.ru

Received 17 March 2014; revision received 15 June 2014
Kvantovaya Elektronika **44** (8) 763–769 (2014)
Translated by M.A. Monastyrskiy

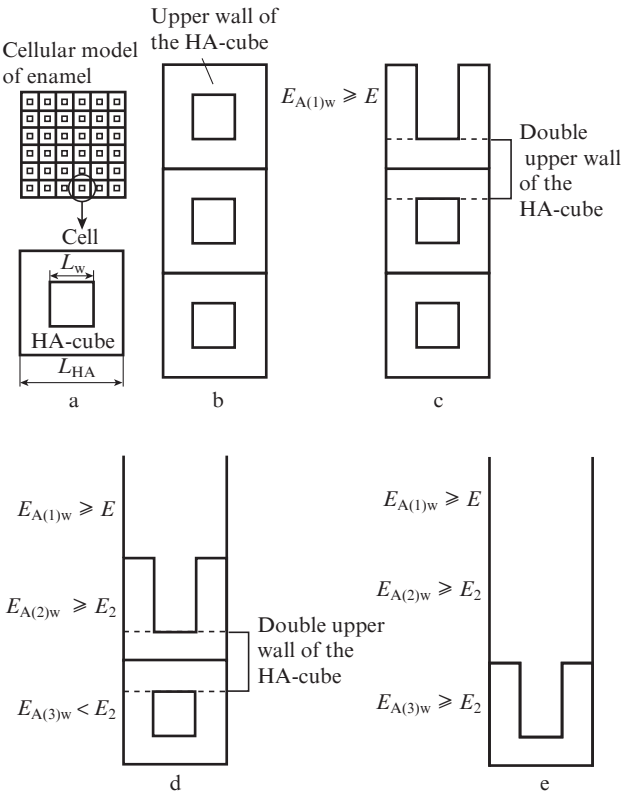

Figure 1. (a) Cellular model of enamel, (b) column of cells, (c) column of cells that contains a cell with the destroyed upper wall of the HA-cube, (d) column of cells with the removed upper cell and a cell with the destroyed upper wall of the HA-cube and (e) column of cells with two removed cells and a cell with the destroyed upper wall of the HA-cube.

lasers [19, 20]. The heating of the tissue that surrounds the ablation area [21] as well as the changes in the absorption coefficient of tissue due to the heating during processing (ablation) [22, 23] are also not taken into account. The cells are isolated from each other, i.e. the model can only be used for erbium laser pulses, whose duration does not exceed the thermal relaxation time of the cell [21], which can be estimated [24] as

$$\tau_r = \frac{z^2}{a}, \tag{1}$$

where z is the cell dimension, ($z = L_{HA} = 5$ μm); and $a = 4.69 \times 10^{-7}$ m^2 s^{-1} is the enamel's thermal conductivity [25].

The value of τ_r, calculated according to (1), in this case is about 50 μs. Thus, this model can be used for the laser pulses whose duration does not exceed 50 μs, or for the pulses consisting of the sequences of micropulses, the duration of each being less than 50 μs. It should be noted that for the most of erbium lasers operating in the free-running mode, the pulse consists of a series of micropulses with duration of ~1 μs, following each other with a repetition rate of 5–10 μs [26].

The water contained in the W-cube, effectively absorbs radiation at the wavelengths of erbium lasers [16] and is heated under the laser radiation. Hydroxyapatite of the HA-cube absorbs the radiation from erbium lasers not so effectively [16]. As a result of heating, the water in the W-cube expands and begins to put pressure on the walls of the HA-cube. It should be noted that the coefficient of the volumetric water expansion {$\alpha = (18-133) \times 10^{-5}$ K^{-1} [27]} is greater than the coefficient of the volumetric expansion of hydroxyapatite (1.1×10^{-5} K^{-1} [28]). The stresses arise in the walls of the HA-cube that surround the W-cube, being dependent on the force F_w [29] that presses against the HA-cube walls and, in turn, depends on the temperature [27], and hence – on the value of the absorbed laser energy E [27]:

$$F_w = \frac{\alpha}{6\chi}\Delta T S_w, \tag{2}$$

$$E = c_w m_w \Delta T, \tag{3}$$

where $\chi = 45 \times 10^{-11}$ Pa^{-1} is the compressibility of water [27]; ΔT is the excess of the water temperature compared to the body temperature; S_w is the surface area of the W-cube wall; c_w is the specific heat of water; and m_w is the W-cube mass.

It is believed in the framework of the cellular model of photomechanical ablation that the enamel ablation occurs if the maximum stress exceeds the tensile strength of hydroxyapatite at break (~40 MPa [30, 31]). In this case, the HA-cube walls surrounding the W-cube are destroyed, and the breakdown products are transferred into environment.

If a single laser pulse with the energy evenly distributed in the beam cross section falls onto the enamel surface, the cellular model allows consideration of the interaction with a single column of cells (Fig. 1b). In this case, the destroying of enamel (of cells) occurs sequentially (in layers).

If the amount of the absorbed energy $E_{A(1)w}$ is large enough to destroy just a single HA-cube (one layer), only its upper wall turns out destroyed and a layer with a microrelief is formed. Figure 1c shows the HA-cube with the upper wall destroyed.

If the removal of two cells (of HA-and W-cubes) occurs sequentially, the side walls of the upper HA-cube turns out destroyed while the upper wall of the lower HA-cube becomes twice as thick (Figs 1c and 1d). The detailed modelling of the ablation in layers is performed in [13, 14]. For modelling of the enamel and calculating of the stresses in the HA-cube walls, the SolidWorks®Premium 2012 software (Adobe Systems Inc., USA) was used. In this case, the force F_w (2) acting on the walls of the HA-cube at different temperatures was initially calculated, and then, in the framework of a three-dimensional model created in SolidWorks, this force was applied to the HA-cube walls from the inner side. The following parameters of hydroxyapatite were used in calculations: modulus of elasticity (Young's modulus) – 90 GPa [32–36], Poisson's ratio (the ratio of shear strain) – 0.28 [16], density – 3.16 g cm^{-3} [16] and shear modulus – 41.8 GPa [37]. As a result, the stresses according to von Mises were calculated [29, 38].

It was assumed that, if the stresses in the upper wall of the HA-cube exceed the tensile strength of hydroxyapatite at break, the upper wall collapses. In this way, the temperature in the W-cube, required for destroying of a single or double wall of the HA-cube, was determined, and, in accordance with these temperatures, the laser energy required to heat the water to the desired temperature (3) was calculated.

The model takes into account that, during the passage of each layer of cells, laser radiation is attenuated according to the Bouguer–Lambert–Beer law [39]:

$$E_{T(n)} = E_0 \exp(-\mu L_{HA} n), \tag{4}$$

where $E_{T(n)}$ is the energy passed through the nth layer of cells; E_0 is the energy of incident laser radiation; and μ is the absorption coefficient of the enamel (cell).

The model also takes into account the contribution of the absorption coefficients of hydroxyapatite and water to the absorption of enamel (cell):

$$E_{A(n)} = E_0\left[\frac{\exp(\mu L_{HA}) - 1}{\exp(\mu L_{HA} n)}\right] = E_{A(n)w} + E_{A(n)HA}. \quad (5)$$

Here, $E_{A(n)}$ is the energy absorbed by the nth layer (cell); $E_{A(n)w}$ is the energy absorbed by water in the nth layer (W-cube); and $E_{A(n)HA}$ is the energy absorbed by hydroxyapatite in the nth layer (HA-cube).

The absorption coefficient of enamel (cell) is calculated as follows:

$$\mu = \mu_w + \mu_{HA}; \quad (6)$$

it constitutes 1666 cm^{-1}, which correlates with the absorption coefficient of the intact enamel, experimentally measured in [22].

The energies $E_{A(n)w}$ and $E_{A(n)HA}$ depend on the volume of the cubes (the W-cube volume constitutes 11% of the total cell volume; the HA-cube volume is 87%):

$$E_{A(n)w} = E_{A(n)}\frac{\mu_w}{\mu}, \quad (7)$$

$$E_{A(n)HA} = E_{A(n)}\frac{\mu_{HA}}{\mu}, \quad (8)$$

where $\mu_w = \mu_{w0}V_w/V_{el}$ is the coefficient of water absorption in the cell; μ_{w0} is the water absorption coefficient (12250 cm^{-1} [16]); V_w is the W-cube volume; V_{el} is the cell volume; $\mu_{HA} = \mu_{HA0}V_{HA}/V_{el}$ is the absorption coefficient of hydroxyapatite in the cell; μ_{HA0} is the absorption coefficient of hydroxyapatite (300 cm^{-1} [16]); and V_{HA} is the HA-cube volume.

As a result of the calculations [14], it was found that, for destroying one of the upper walls of the HA-cube, it is necessary to heat the water to a temperature of +150 °C, herewith the force (2), which is required for destroying, amounts to 2.5×10^{-4} H, the energy (3), which is absorbed in the W-cube, – to 6.6 nJ, and the energy (5), (7), which is absorbed in the cell, – to 13.9 nJ. Destroying of the double upper wall of the HA-cube occurs when the water temperature reaches +290 °C. In this case, the force (2), which is required for destroying, amounts to 10.1×10^{-4} H, the energy (3), which is absorbed in the W-cube, – to 14.7 nJ, and the energy (5), (7), which is absorbed in the cell, – to 30.9 nJ.

When modelling the destroying of enamel by a laser, it was assumed that if the energy absorbed in the cell drops below 30.9 nJ, the destruction stops and the geometry shown in Figs 1d and 1e turns out fixed.

By transforming expression (5), we can calculate the number of layers n that have been removed during a single pulse or a micropulse from a train, including the last layer with a microrelief, as well as the ablation depth h versus the density W_E of the radiation energy that falls onto the area with the transverse dimension equal to the size of a single HA-cube [13]:

$$n = \frac{1}{\mu L_{HA}}\ln\left\{[\exp(\mu L_{HA}) - 1]\frac{\mu_w L_{HA}^2 W_E}{\mu E_2}\right\}, \quad (9)$$

$$h = nL_{HA} - \frac{L_{HA} - L_w}{2}, \quad (10)$$

where E_2 is energy to be absorbed in the W-cube for destroying the double wall of the HA-cube; L_w is the edge length of the W-cube; and $L_{HA}^2 W_E$ is the incident radiation energy E_0.

If laser radiation having a Gaussian energy distribution in the beam cross section falls onto the enamel surface, the number of layers removed during a single pulse in the cellular model (a micropulse from a train) will depend, in each column of cells, on the energy that corresponds to this column:

$$n(x,y) = \frac{1}{\mu L_{HA}}\ln\left\{[\exp(\mu L_{HA}) - 1]\frac{\mu_w E_{el}(x,y)}{\mu E_2}\right\}, \quad (11)$$

where $E_{el}(x,y)$ is the energy of radiation incident on each cell, varying according to the Gaussian distribution. Based on the expressions proposed in the Supplement to [40], the expression for the energy that corresponds to the cell of size L_{HA} can be written as follows:

$$E_{el}(x,y) = L_{HA}^2\frac{E_0}{2\pi\sigma_a^2}\exp\left\{-\frac{[r(x,y)]^2}{2\sigma_a^2}\right\}, \quad (12)$$

where x and y are the coordinates that define the position of the cell centre relative to the beam centre; and $r(x,y)$ is the distance between the beam and cell centres. In this case,

$$\sigma_a^2 = \sigma^2 + \frac{1}{12}L_{HA}^2, \quad (13)$$

where σ is the width of the Gaussian distribution (half the radius according to the e^{-2} level).

The calculations according to (11) and (12) were carried out in the MatLab (The MathWorks Inc., USA) environment; the result of calculation is two-dimensional arrays $E_{el}(x,y)$ and $n(x,y)$. Figure 2 demonstrates the energy distribution for the beam with E_0 = 1 mJ, 2σ = 30 μm, obtained according to (12).

Figure 3 shows the microcrater profile in enamel, calculated in accordance with the above-described cellular model as a result of irradiation by the YAG:Er laser with a Gaussian energy distribution [the beam radius 30 μm at the level e^{-2} (2σ), the energy E_0 = 1 mJ], as well as a photograph of the longitudinal cross section of the microcrater formed in the human tooth enamel when exposed to a single pulse of a free-running single-mode YAG:Er laser (λ = 2.94 μm) with the duration of $\tau_p = 100 \pm 10$ μs and the energy of E_0 = 1 mJ [41]. Note that the pulse of a free-running YAG:Er laser consisted of a train of micropulses with the duration of each $\tau_{pm} \sim 1$ μs and the time interval between the pulses ~10 μs. Consequently, *albeit* $\tau_p > \tau_r$, it is evident that the laser impact occurs only during the micropulse action, i.e. during the time $\tau_{pm} < \tau_r$. Thus, the previously formulated condition that the photomechanical cellular model is applicable for the laser pulses with $\tau_p \leqslant 50$ μs is fulfilled in this case.

4. Simulation of the texture surface area in the enamel after its micromachining by means of erbium laser radiation

Figure 4a shows a flat surface XY that can be used to describe an untreated enamel surface. After laser micromachining, it can be represented by a set of fragments of a flat surface and

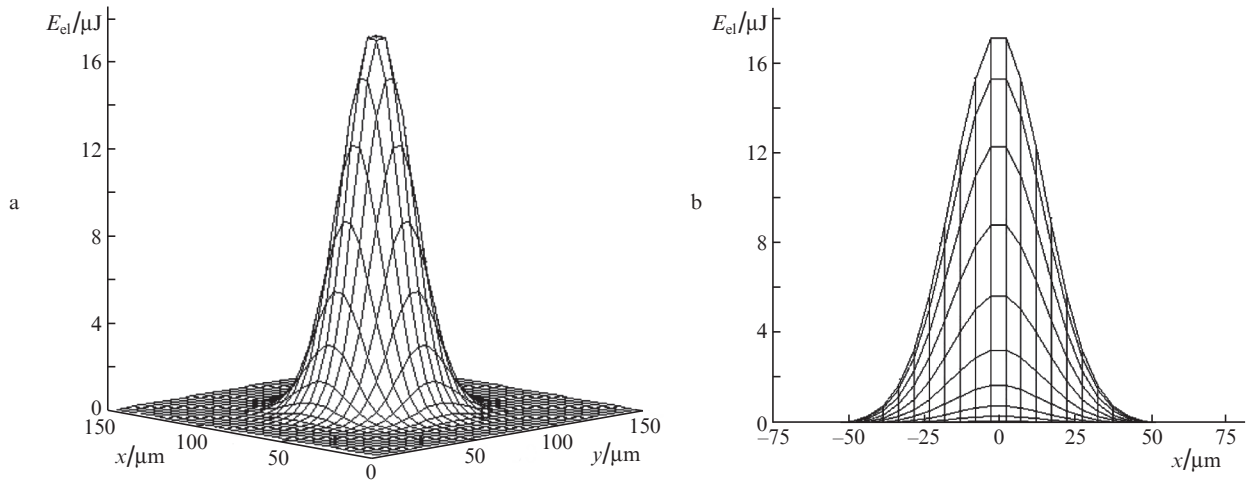

Figure 2. (a) Three-dimensional and (b) two-dimensional distribution of the energy incident on the enamel surface (E_0 = 1 mJ, 2σ = 30 μm).

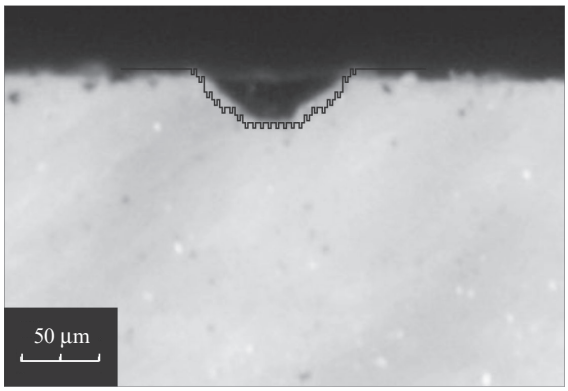

Figure 3. Calculated profile of a microcrater in the enamel (black line) and the picture of a longitudinal section of a microcrater obtained in the experiment (YAG:Er laser, λ = 2.94 μm, τ_p = 100 ± 10 μs, E_0 = 1 mJ).

microcraters – radial texture (Fig. 4b). The microcraters in the cellular photomechanical ablation model have a complex shape (Fig. 4c).

If a single pulse with a uniform energy distribution in the beam cross section falls on the enamel surface, and the amount of the absorbed energy is large enough to destroy just the upper wall of the HA-cube, the surface area of the cell that is not destroyed completely and contains a microdefect (for a single surface), in the framework of the cellular model can be estimated as

$$S_{m0} = L_{HA}^2 + 4L_w\left(\frac{L_{HA} - L_w}{2} + L_w\right). \quad (14)$$

It is easy to calculate that in this case the surface area is increased by 2.4 times compared to the flat surface area.

If a single pulse with a Gaussian energy distribution in the beam cross section falls onto the enamel surface, the microcrater surface area in the framework of the cellular model will depend on the number of layers removed in each column of cells. Figure 5 shows the marked vertical surfaces, or the surfaces with a microrelief, the sum of surface areas of which gives the entire surface area of the whole microcrater.

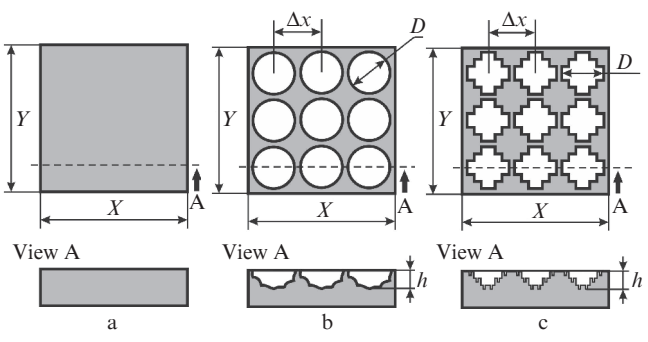

Figure 4. Schemes of the enamel surface relief: (a) unprocessed surface, (b) radial texture and (c) texture corresponding to the cellular photomechanical ablation model; Δx is the micromachining step (the distance between the centres of the craters) and D is the microcrater diameter.

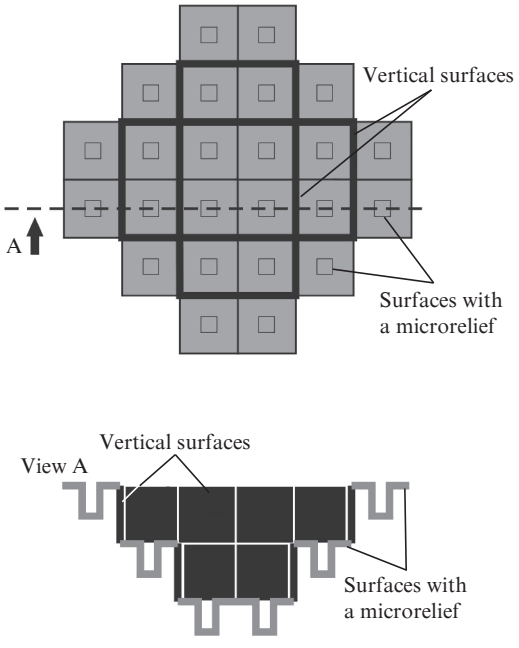

Figure 5. Structure of the microcrater surface corresponding to the cellular photomechanical ablation model.

The surface area of a single crater and the surface area comprising the texture depend on the number of the cell layers removed in each column of cells, i.e. depend on the depth that, in turn, is conditioned by the magnitude of the energy incident onto the enamel surface and the peculiarities of its distribution in space. The crater can be formed by exposing the enamel to a train of laser pulses (micropulses from a train). The area S_{cm} of a single microcrater with a relief is calculated as follows:

$$S_{cm} = S_{vm} + S_m, \tag{15}$$

$$S_m = S_{m0}N_m, \tag{16}$$

$$S_{vm} = L_{HA}^2 N_v, \tag{17}$$

where S_{vm} is the area of vertical surfaces in the microcrater; S_m is the area of the microcrater surfaces with a relief; N_v is the number of vertical surfaces in the microcrater; and N_m is the number of cells with a relief in the microcrater.

It should be noted that, using a program created in MatLab, N_m was calculated as a number of the nonzero elements in the array $n(x,y)$ (11), N_v – as a sum of differences of the values in columns (and rows) of the array $n(x,y) - 1$. The method described is applicable for calculating both the surface area of a single microcrater, and the surface area comprising several craters in any of their position relative to each other.

Consider a flat area of size $L_0 \times L_0$ on the enamel surface. If the area is smooth (no micromachining by laser beam), its area is $S_0 = L_0^2$. If a texture with different steps Δx is formed on the enamel surface as a result of micromachining, the ratio of the step Δx to the microcrater diameter D can be denoted as $k = \Delta x/D$. The surface area of the texture S_k depends on k. For $k < 1$, the surface texture is formed as a result of superposition of the microcraters (Fig. 6a), for $k \geqslant 1$, the texture can be considered as a set of isolated microcraters (Figs 6b and 6c).

The area of the texture surface in the enamel after micromachining was calculated by using a programme created in MatLab. In modelling, we specified a coordinate system defining the position of the cell centres on an area measuring $L_0 \times L_0$ and a coordinate system for the laser pulse energy distribution in the cells. After that the array $n(x,y)$ was calculated for the original position of the laser beam, and thus the formation of a single microcrater in the area was simulated. Further, the coordinate system that had been defined for the energy distribution was shifted at the distance Δx in the coordinate system defined for the $L_0 \times L_0$ area. Thus, the sequential formation of the craters in the area with different Δx and, accordingly, with different k, was modelled. In this case, a sequential summation of the array values $n(x,y)$ was conducted with an offset, which allowed one to realise the superposition of the microcraters for $k < 1$. The number N_{vk} of the vertical surfaces and the number N_{mk} of the surfaces with a relief, which are necessary to calculate the total surface area of the texture, were calculated by the above method. The surface area of the texture was determined as follows:

$$S_{vk} = L_{HA}^2 N_{vk}, \tag{18}$$

$$S_{mk} = S_{m0}N_{mk}, \tag{19}$$

$$S_k = S_0 - N_{mk}L_{HA}^2 + (S_{vk} + S_{mk}), \tag{20}$$

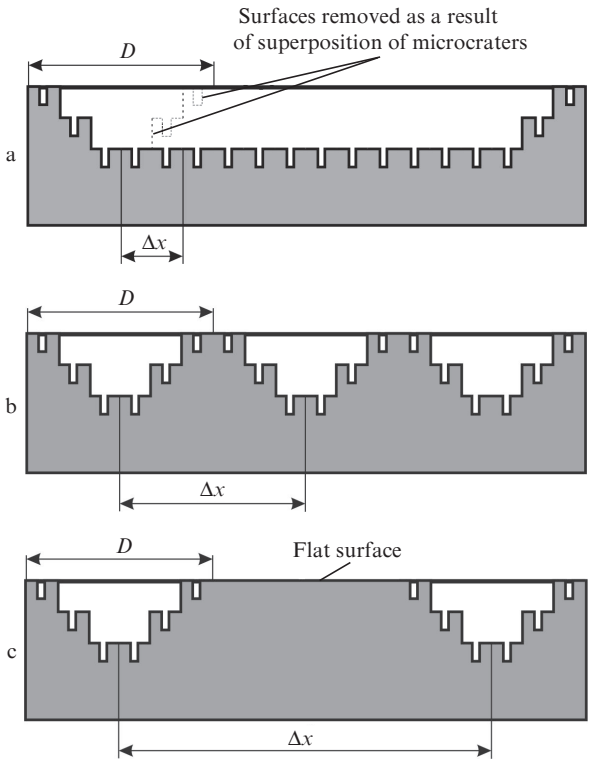

Figure 6. Structure of the surface texture formed at (a) $k < 1$, (b) $k = 1$ and (c) $k > 1$.

where S_{vk} is the area of vertical surfaces in the texture; S_{mk} is the area of the microcrater surfaces with a microrelief in the texture; N_{vk} is the number of vertical surfaces in the texture; and N_{mk} is the number of the surfaces with microrelief in the texture.

Herewith, the area S_0 of the flat surface was calculated with regard to the actual number of the microcraters that can fit on the area of approximately 1×1 mm.

5. Simulation of the full work of adhesion on the surface texture in the enamel after its micromachining by erbium laser radiation

According to [42, 43], the full work of adhesion is related to the area of contacting adhering materials. For a flat surface, the full work of adhesion is

$$W_0 = W_a S_0, \tag{21}$$

where W_a is the work of adhesion attributable to a unit surface.

For the surfaces containing a texture, the full work of adhesion W_k is calculated as follows:

$$W_k = W_a S_k, \tag{22}$$

where S_k is the texture surface area (after micromachining), see (20).

Then the normalised full work of adhesion resulted from micromachining can be considered as the area ratio:

$$\frac{W_k}{W_0} = \frac{S_k}{S_0}. \tag{23}$$

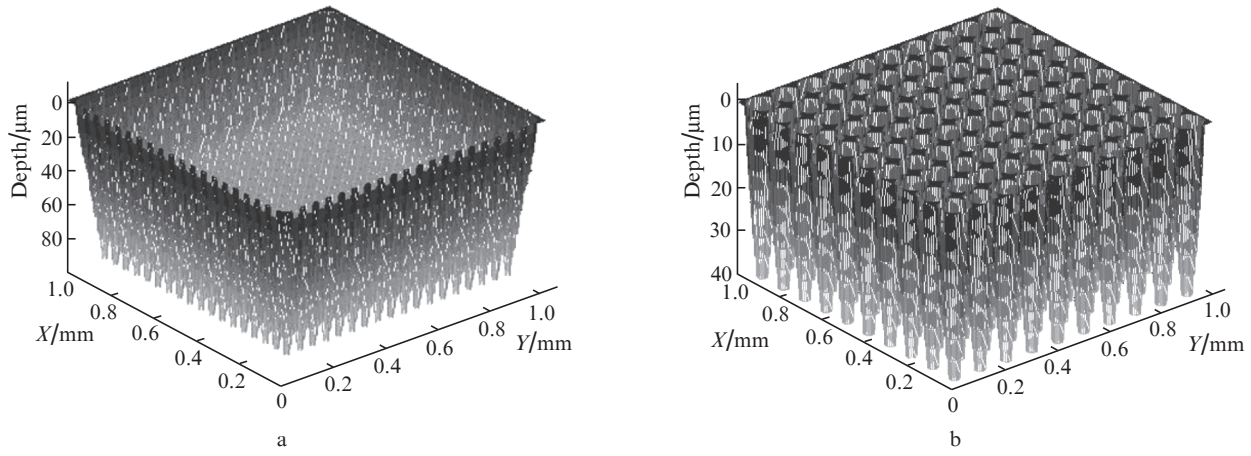

Figure 7. Texture calculation results for $E_0 = 1$ mJ, $2\sigma = 30$ μm at (a) $k = 0.5$ and (b) 1.

It should be noted that at $k < 1$, the superposition of craters leads to creation of a texture with the depth that exceeds the depth of the microcrater, and it is incorrect to describe the changes in the area of this texture by using S_0, because in this case a cavity is formed (Fig. 7a), the area of which, in the absence of the texture, differs from S_0. At $k \geqslant 1$, the texture depth does not exceed the depth of a single crater, and in this case the comparison with S_0 is justified (Fig. 7b).

Figure 8 represents the dependence of the normalised full work of adhesion W_k/W_0 on the coefficient k, which is calculated in the framework of the above-described cellular photomechanical ablation model for the case of micromachining of a flat surface by the radiation from erbium laser at $k \geqslant 1$.

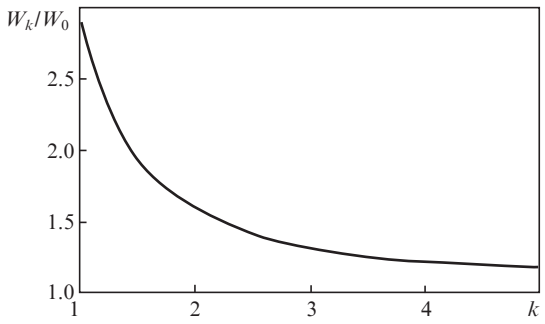

Figure 8. Dependence of W_k/W_0 on k calculated in accordance with the cellular photomechanical ablation model ($E_0 = 1$ mJ, $2\sigma = 30$ μm, $X = Y = 1$ mm).

It can be seen that the greatest increase in the full work of adhesion ($W_k/W_0 = 2.9$) after the laser micromachining (for a surface containing a texture) compared to W_0 is observed at $k = 1$. With increasing distance between the craters, the texture surface area decreases. The authors of paper [4] describe an experiment on studying the bond strength to the enamel surface after the micromachining with the use of a highly flowable, light-cure composite material 'Revolution' (Kerr, Germany). A 2.94-μm single-mode, free-running YAG:Er laser was employed for the micromachining with a step equal to the micro-crater diameter. The radiation energy in the processing area was 1 mJ (±3.5%), the laser pulse FWHM duration constituted 100 μs (±10%). Each microcrater in the texture was formed by the action of a single pulse of free-running lasing in non-contact mode. It was established that the bond strength of 'Revolution' (Kerr, Germany) with the surface comprising the texture formed by the laser radiation is three times higher than that with the surface without such a texture.

Thus, the result of calculation performed in the framework of the cellular photomechanical ablation model is in good agreement with the data obtained in the experiment [4]. It should be emphasised that the inconsistency in the adhesion behaviour after the laser processing, that have been mentioned earlier in the analysis of the literature [5–11], may be related to the two following factors: firstly, the lack of the proper control for the parameter k on the part of researchers, that, as can be seen from Fig. 8, has a significant impact on the area S_k, and secondly, the use of the viscous filling materials that are not capable of flowing into the micro-defects created on the enamel surface during laser irradiation.

Thus, in this paper a 3D cellular model of the human tooth enamel and a photomechanical cellular model of its ablation are described. For the first time, within the framework of the cellular photomechanical ablation model, a simulation of the surface area and the full work of adhesion surface texture in the enamel after its micromachining by means of erbium laser radiation have been carried out. The results of calculations show that the full work of adhesion depends on the distance between the centres of microcraters in the texture and attains its maximum when the distance between the centres becomes equal to the microcrater diameter. The results of simulation are in a good agreement with the experimental data.

References

1. Coluzzi D.J., Convissar R.A. *Atlas of Laser Applications in Dentistry* (Hanover Park, IL: Quintessence Publ. Co, Inc., 2007).
2. Walsh L.J. *Aust. Dent. J.*, **48** (3), 146 (2003).
3. Convissar R.A. *Principles and Practice of Laser Dentistry* (St. Louis, MO: Mosby Elsevier, 2011).
4. Belikov A.V., Pushkaryova A.E., Skripnik A.V., Strunina T.V., Schatilov K.V. *Izv. Vyssh. Uchebn. Zaved., Ser. Priborostr.*, **53** (4), 52 (2010).
5. Samad-Zadeh A., Harsono M., Belikov A., Shatilova K., Skripnik A., Stark P., Egles C., Kugel G. *Dental Materials*, **27** (10), 1038 (2011).
6. Gardner A.K., Staninec M., Fried D. *Proc. SPIE Int. Soc. Opt. Eng.*, **5687**, 144 (2005)
7. Eguro T., Maeda T., Ishizaka Y., Takahashi K., Suzuki T., Tanaka H., Katsuumi I. *Intern. Congr. Ser.*, **1248**, 157 (2003).

8. Başaran G., Hamamcı N., Akkurt A. *Lasers Med. Sci*., **26**, 149 (2011).
9. Shahabi S., Bagheri H.G., Ramazani K. *Lasers Med. Sci*., **27**, 371 (2012).
10. Başaran E.G., Ayna E., Başaran G., Beydemir K. *Lasers Med. Sci*., **26**, 13 (2011).
11. Dunn W.J., Davis J.T., Bush A.C. *Dental Mater*., **21**, 616 (2005).
12. Belikov A., Vostryakov R., Skrypnik A., Shatilova K. *Techn. Digest, 5th Finnish-Russian Photonics and Laser Symposium* (S.-Petersburg, 2011) p. 91.
13. Belikov A.V., Shatilova K.V., Skrypnik A.V., Vostryakov R.G., Maykapar N.O. *Proc. SPIE Int. Soc. Opt. Eng*., **8221**, 82210K (2012).
14. Belikov A.V., Shatilova K.V., Skrypnik A.V. *Proc. SPIE Int. Soc. Opt. Eng*., **8929**, 89290A (2014).
15. Hibst R., Keller U. *Proc. SPIE Int. Soc. Opt. Eng*., **1880**, 156 (1993).
16. Verde A.V., Ramos M.M.D. *Proc. SPIE Int. Soc. Opt. Eng*., **5687**, 69 (2005).
17. Fejerskov O., Kidd E. (Eds) *Dental Caries: The Disease and its Clinical Management* (Oxford: Blackwell Munksgaard, 2008).
18. Nanci A. *Ten Cate's Oral Histology: Development, Structure, and Function* (Saint Louis: Mosby, 2003).
19. Featherstone J.D.B., Rechmann P., Fried D. *Proc. SPIE Int. Soc. Opt. Eng*., **910**, 136 (2000).
20. Fried D., Visuri S.R., Featherstone J.D.B., Walsh J.T., Seka W., Glena R.E., McCormack S.M. *J. Biomed. Opt*., **1** (4), 455 (1996).
21. Majaron B., Lukac M. *Proc. SPIE Int. Soc. Opt. Eng*., **3593**, 184 (1999).
22. Belikov A.V., Skripnik A.V., Schatilov K.V. *Opt. Spektrosk*., **109** (2), 1297 (2010).
23. Vodop'yanov K.L. *Zh. Eksp. Teor. Fiz*., **97**, 205 (1990).
24. Rakitin O.I. *Vestnik TGTU*, **10**, 166 (2004).
25. Brown W.S., Dewey W.A., Jacobs H.R. *J. Dent. Res*., **49**, 752 (1970).
26. Altshuler G.B., Belikov A.V., Gagarskiy S.V., Erofeev A.V., Parakhuda S.E. *Proc. SPIE Int. Soc. Opt. Eng*., **1984**, 190 (1995).
27. Kikoin I.K. (Ed.) *Tablitsy fizicheskikh velichin* (Tables of Physical Quantities) (Moscow: Atomizdat, 1976).
28. Santin M. *Strategies in Regenerative Medicine: Integrating Biology with Materials Design* (New York: Springer Science, Business Media, 2009).
29. Pisarenko G.S. (Ed.) *Soprotivlenie materialov: Uchebnik dlya Vuzov* (Strength of Materials: Textbook for High Schools) (Kiev: Vishcha Shkola, 1979).
30. Müller R.T., Patsalis T. *Archives of Orthopaedic and Trauma Surgery*, **116**, 334 (1997).
31. Komlev V.S., Barinov S.M. *J. Mater. Sci.: Mater. Medicine*, **13**, 295 (2002).
32. Kinney J.H., Marshall S.J., Marshall G.W. *Critical Rev. Oral Biol. & Med*., **14**, 13 (2003).
33. Padilla S., Vallet-Regı M., Ginebra M.P., Gil F.J. *J. Europ. Ceramic Soc*., **25**, 375 (2005).
34. Teraoka K., Ito A., Maekawa K., Onuma K., Tateishi T., Tsutsumi S. *J. Dental Res*., **77**, 1560 (1998).
35. Lopes M.A., Silva R.F., Monteiro F.J., Santos J.D. *Biomater*., **21**, 749 (2000).
36. Verde A.V., Ramos M.M.D. *Proc. SPIE Int. Soc. Opt. Eng*., **5687**, 69 (2005).
37. Lopes M.A., Silva R.F., Monteiro F.J., Santos J.D. *Biomater*., **21**, 749 (2000).
38. Nadai A. *Theory of Flow and Fracture of Solids* (New York: McGaw-Hill, 1963).
39. Niemz M.H. *Laser – Tissue Interactions: Fundamentals and Applications* (Berlin: Springer, 1996).
40. Mortensen K.I., Churchman L.S., Spudich J.A., Flyvbjerg H. *Nat. Meth*., **7**, 377 (2010).
41. Belikov A.V., Skrypnik A.V., Shatilova K.V. *Proc. SPIE Int. Soc. Opt. Eng*., **7376**, 73760D (2010).
42. Berlin A.A., Basin V.E. *Osnovy adgezii polimerov* (Fundamentals of Polymer Adhesion) (Moscow: Khimiya, 1974).
43. Van Noort R. *Introduction to Dental Materials* (London: Mosby, 2002).